

Shot noise in self-assembled InAs quantum dots

A. Nauen,^{1,*} I. Hapke-Wurst,¹ F. Hohls,¹ U. Zeitler,¹ R. J. Haug,¹ and K. Pierz²

¹*Institut für Festkörperphysik, Universität Hannover, Appelstr. 2, D-30167 Hannover, Germany*

²*Physikalisch-Technische Bundesanstalt, Bundesallee 100, D-38116 Braunschweig, Germany*

(Dated: October 28, 2018)

We investigate the noise properties of a GaAs-AlAs-GaAs tunneling structure with embedded self-assembled InAs quantum dots in the single-electron tunneling regime. We analyze the dependence of the relative noise amplitude of the shot noise on bias voltage. We observe a non-monotonic behaviour of the Fano-factor α with an average value of $\alpha \approx 0.8$ consistent with the asymmetry of the tunneling barriers. Reproducible fluctuations observed in α can be attributed to the successive participation of more and more InAs quantum dots in the tunneling current.

PACS numbers: 73.63.Kv, 73.40.Gk, 72.70.+m

Performing noise measurements on microscopic semiconductor devices allows an insight into details of the transport process not accessible by conventional conductance experiments. In the most simple system for such an experiment, an ideal tunneling barrier, a frequency-independent power spectrum of the current noise up to frequencies corresponding to the transit time of the carriers is observed. This case, known as full shot noise, is due to a Poissonian statistics of the individual tunneling events and a totally uncorrelated flow of charge carriers¹.

If an additional source of negative correlation due to the Pauli-exclusion principle is introduced the noise amplitude was shown to be reduced^{2,3}. In these experiments, changing the ratio of the transmissivity through the two barriers of a double-barrier resonant-tunneling structure resulted into a suppression of the relative shot-noise amplitude compared to full shot noise. Theoretical models for purely coherent transport⁴ and for classical sequential tunneling⁵ have been developed. Both yield identical results for the noise suppression since shot noise generally is not sensitive to dephasing⁶. This suppression of the shot noise was also observed for resonant tunneling in zero-dimensional systems^{7,8}. Under certain circumstances a positive correlation between individual tunneling events can even increase the noise power above the full Poissonian shot noise value^{9,10}.

In this paper we present noise measurements on self-assembled InAs quantum dot (QD) systems. These samples form an ideal system for noise experiments since they provide zero-dimensional states of microscopic dimensions. Furthermore, it is possible to select individual QDs for transport by applying different bias voltages between the source and drain contacts^{11,12,13,14}. Consequently, we are able to measure the noise spectra of a resonant tunneling current through single zero-dimensional states.

What we find in the experiments is a modulation of the amplitude of the shot noise normalized to full shot noise as a function of the applied bias voltage V_{SD} . We can link this to resonant single-electron tunneling through individual InAs QDs in agreement with theoretical expectations.

The active part of our samples consists of a GaAs-

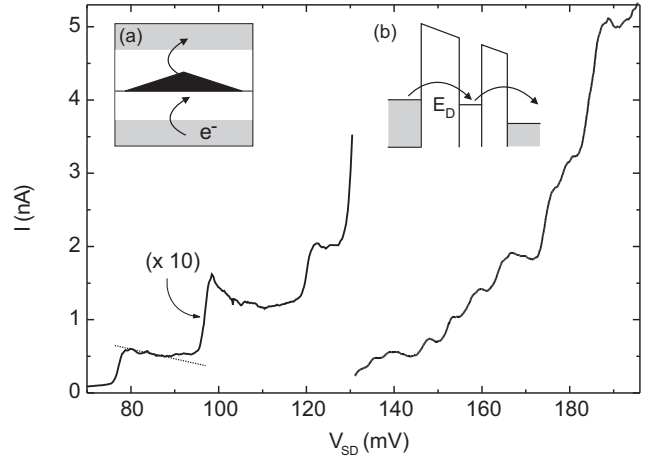


FIG. 1: Current-voltage characteristics of an InAs quantum dot array measured at $T = 1.7$ K. The current for bias voltages below 130 mV is magnified by a factor of 10. The dotted line is a guide to the eye representing the expected current through a single dot.

Insets: (a) Principle sample structure of an InAs QD (black) embedded in an AlAs barrier (white) between two GaAs electrodes (grey). The arrows mark the tunneling direction of the electrons. (b) Schematic profile of the band structure at positive bias where resonant-tunneling through a QD is observed.

AlAs-GaAs resonant tunneling structure with embedded InAs QDs of 10-15 nm diameter and 3 nm height¹⁵. These QDs are situated between two AlAs barriers of nominally 4 nm and 6 nm thickness. The formation of pyramidal QDs is due to the lattice mismatch between InAs and AlAs resulting in a Stranski-Krastanov growth mode. About one million QDs are placed randomly on the area of an etched diode structure of $40 \times 40 \mu\text{m}^2$ area. A 15 nm undoped GaAs spacer layer and a GaAs buffer with graded doping on both sides of the resonant tunneling structure provide three-dimensional collector and emitter electrodes. Connection to the active layer is realized by annealed Au/Ge/Ni/Au contacts.

A schematic sample structure with one InAs QD embedded in an AlAs barrier is sketched in the inset (a) of

Fig. 1. When applying a finite bias the zero-dimensional states of the QDs inside of the AlAs barrier can be populated by electrons and a current through the structure sets on, see Fig. 1 (b). In our experiments a positive bias voltage means tunneling first through the base of a QD and out of the top. Due to the finite height of the InAs QDs of approximately 3 nm their pinnacles penetrate into the top AlAs barrier. This effectively reduces the width of the top barrier below that of the nominally thinner barrier at the base of the QDs. Therefore positive bias voltage corresponds to non-charging transport.

A typical current-voltage (I - V) characteristic is shown in Fig. 1. We observe a step-like increase of the current at bias voltages of 75, 95 and 120 mV. Each one of these current steps corresponds to the emitter Fermi energy E_F getting into resonance with the ground states of different individual QDs. At bias voltages lower than 70 mV no transport occurs since all the zero-dimensional states inside the barrier lie above the emitter Fermi energy E_F and, consequently, electron flow is prohibited by the AlAs barriers.

The negative slope of the first current plateaus is related to the density of states of the three-dimensional emitter. Indeed, a triangular-shaped I - V curve as indicated by the dotted line is expected for such a 3D-0D-3D tunneling diode. In particular with a Fermi energy $E_F = 13.6$ meV and an energy-to-voltage conversion factor of approximately 0.3 the current falls back to zero when the distance to the onset voltage exceeds $\Delta V = 45$ mV¹⁴. Then the QD ground state with energy E_D falls below the conduction band edge E_C of the emitter and no resonant transport through this particular dot can take place anymore.

The noise experiments are performed in a ⁴He bath cryostat with a variable temperature insert. The sample is always immersed in liquid helium. This allows for temperatures between 1.4 K and 4 K under stable conditions.

The bias voltage V_{SD} is applied between the source and drain electrodes by means of a filtered DC-voltage source. The noise signal is detected by a low-noise current amplifier in a frequency range from 0 to 100 kHz. The use of a current amplifier requires small capacitive loading by the external circuit. Accordingly, electrical connection to the sample is provided by a low-capacitance line with $C \approx 10$ pF (see Fig. 2, inset).

The amplifier output is fed into a fast Fourier-transform analyzer (FFT) to extract the noise spectra and in parallel into a voltmeter for measuring the total DC-current through the sample. The amplifier and the input stages of the FFT have been tested for linearity in the range of interest, overall calibration has been verified by measuring the thermal noise of thick film resistors.

By analyzing the frequency spectra we find that shot noise is present above a certain frequency, as shown in Fig. 2. The spectra have been smoothed using a box-car average. The fluctuations of the signal increase with frequency because of the capacitive loading of the current amplifier. The superior signal-to-noise ratio at a

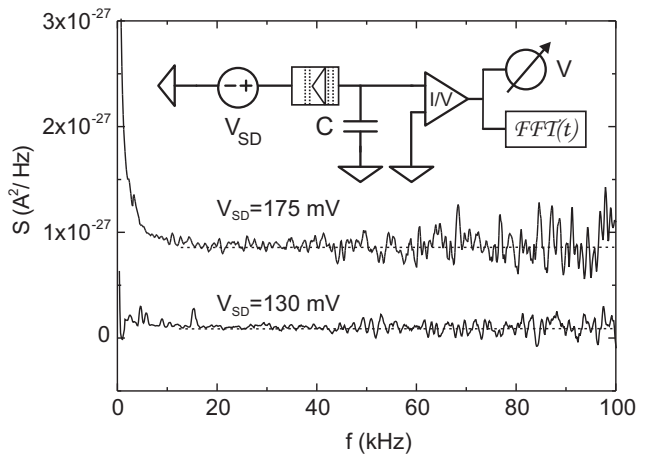


FIG. 2: Typical noise spectra of an array of self-assembled InAs quantum dots for two different bias voltages V_{SD} . The dashed horizontal lines are drawn to stress the absence of any frequency dependence above 20 kHz.

Inset: Schematic of the experimental setup. A DC-voltage source drives a current through the device which is fed into a low-noise current amplifier by means of a low-capacitance cable with $C \approx 10$ pF. The noise spectra are acquired by a fast Fourier-transform analyzer (FFT). Additionally, the DC-part of the current is monitored.

bias voltage $V_{SD} = 130$ mV is due to a higher integration time. At frequencies below ~ 20 kHz we find an additional $1/f$ -noise contribution.

For characterizing the relative amplitude of the shot noise we use the dimensionless Fano factor α , being defined as the ratio $\alpha = S/S_{poisson}$ between full Poissonian shot noise $S_{poisson} = 2eI$ (for $eV_{SD} \gg k_B T$) and the measured noise power density S , with the total current I and the electron charge e . Consequently, full shot noise corresponds to $\alpha = 1$. For the purpose of extracting α from the spectra we average above the cut-off frequency of the $1/f$ noise, thus increasing the signal to noise ratio. The measured shot noise S as a function of bias voltage V_{SD} is shown in Fig. 3. For comparison we plot the calculated full shot noise $\alpha = 1$.

We consider the bias range where the first three QD states get into resonance with the emitter Fermi energy E_F as depicted in Fig. 3. By averaging current and noise on the first plateau we find a Fano factor $\alpha \approx 0.8$. The suppression of shot noise for on-resonance tunneling is well understood theoretically (see⁶ and references therein): The value of the Fano factor α is directly linked to the transmissivity aspect of left and right barrier:

$$\alpha = \frac{\Gamma_L^2 + \Gamma_R^2}{(\Gamma_L + \Gamma_R)^2}. \quad (1)$$

Γ_L and Γ_R are the partial decay widths of the resonant state E_D . For symmetric barriers ($\Gamma_L = \Gamma_R$) the suppression would become $\alpha = 1/2$. Responsible for this is the Pauli exclusion principle: For symmetric barriers the

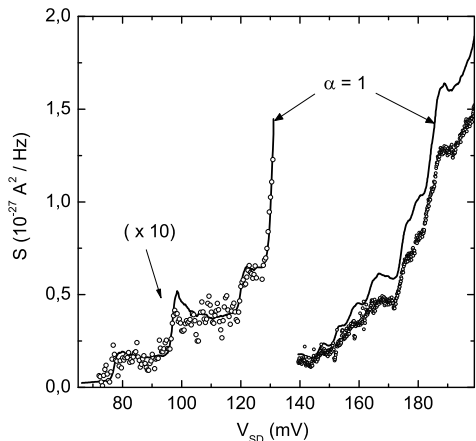


FIG. 3: Measured shot noise (open circles) of the InAs QD diode. For comparison the calculated full shot noise ($\alpha = 1$) is plotted (black curve). The data for bias voltages smaller than 130 mV have been scaled with a factor of 10. Additionally, a 7-point boxcar average has been applied (the voltage resolution of the original data is $\Delta V_{SD} = 0.2$ mV).

tunneling of an electron from the emitter into the QD is forbidden as long as the QD state E_D is occupied. This anti-correlates successive tunneling events. However, in the asymmetric case (e.g. $\Gamma_L \gg \Gamma_R$) full poissonian shot noise ($\alpha = 1$) would be recovered, since then the transport will be controlled by one barrier solely.

To get a more quantitative insight we use the textbook formula for the transmission coefficient T of a rectangular tunneling barrier neglecting any influence of the applied bias voltage on the shape of the barrier potential:

$$T(E) = \frac{1}{1 + \left\{ 1 + \left(\frac{1}{4} \left(\frac{\kappa}{k} - \frac{k}{\kappa} \right)^2 \right) \right\} \sinh^2(\kappa a)}, \quad (2)$$

with $\kappa = \sqrt{2m^*(V_0 - E)}/\hbar$ and $k = \sqrt{2m^*E}/\hbar$, the barrier width a and height $V_0 = 1.05$ eV $- E_F$, the effective electron mass m^* and the energy E of the tunneling emitter electrons. This is justified since the AlAs barriers in our sample are narrow but high. The transmission coefficients $T_{L,R}$ of the left and right barrier are linked to the partial decay widths $\Gamma_{L,R}$ via $T_{L,R} = \hbar\nu T_{L,R}$ with the attempt rate $\nu = \sqrt{2E_D/m^*}/w$ of the resonant QD state E_D and w the distance between both barriers. Since ν is identical for both barriers Eq. (1) transforms into

$$\alpha = \frac{T_L^2 + T_R^2}{(T_L + T_R)^2}. \quad (3)$$

We take the thickness of the tunneling barrier at the base of the QD $a_L = 4$ nm as fixed. From the measured Fano factor $\alpha \approx 0.8$ we extract from Eq. (3) the ratio $T_R/T_L = 8.4$ at a bias voltage of 0.1 V. We can now use Eq. (2) to calculate the thickness of the second barrier as $a_R = 3.2$ nm. The top AlAs barrier has been grown

with a nominal thickness of 6 nm and the average height of an InAs QD is 3 nm. Hence, the calculated value of $a_R = 3.2$ nm is in good agreement with the expected barrier thickness of 3 nm.

Up to now we have dealt with the bias regime where very few single QDs determine the transport. If the bias voltage is increased above 130 mV the energy separation between consecutive QD states is narrowed considerably (Fig. 3) compared to the onset region. Therefore, the number of QD states contributing to the current reaches the order of ten at 190 mV. In this multiple-QD tunneling regime we observe a non-monotonic behaviour of the Fano factor with the noise being sub-Poissonian ($\alpha < 1$) on resonance. In between the current plateaus we find increasing noise. However, there α is found to be still sub-poissonian. For better insight into this observation we have plotted the corresponding Fano factor α in comparison with the I - V characteristics in Fig. 4 (a).

First, we will concentrate on the increase of the Fano factor α at the onset of every current plateau (see Fig. 4(a)). A detailed view of the Fano factor at a current step is plotted in Fig. 4 (b). Full Poissonian shot noise is present in a stream of electrons that is totally uncorrelated. The suppression of the shot noise for on-resonance transport as predicted by Eq. (1) is due to a negative correlation in the electron flow induced by the Pauli exclusion principle: As one electron enters the resonant QD state the tunneling of further electrons into that state is forbidden. The resulting dependence between consecutive tunneling events suppresses the noise.

When a QD level starts coming into resonance only a few electrons from the high energy tail of the Fermi distribution contribute to the resonant current. This implies that the Pauli principle does not play a role as long as an electron in the QD can tunnel out before the next one is available in the emitter, in other words as long as the attempt frequency in the emitter is smaller than the tunneling rate through the second barrier. In such an uncorrelated case the Fano factor will approach its Poissonian value $\alpha = 1$, see Fig. 4 (b). If the resonant state is moved further into the Fermi sea of the emitter, the number of electrons available to resonant tunneling increases and the Pauli principle sets in. The Fano factor starts becoming suppressed until reaching its minimum on the current plateau.

Applying higher bias voltage we note in Fig. 4 (a) a reduction of the overall modulation amplitude in the Fano factor α , eventually leading to an average suppression of $\alpha \approx 0.8$. As we have stated above every single QD contributes to the total current over a bias range of approximately 50 mV. This implies that e.g. the QD linked to the current step at $V_{SD} = 145$ mV in Fig. 4 (a) transmits electrical current over most part of the plotted bias range (up to 190 mV) before its eigenstate moves below the emitter conductance band edge E_c . The same holds for every consecutive QD. Thus at a specific bias voltage V_{SD} the total current $I_{total}(V_{SD})$ is a sum of the currents I_i through every single QD :

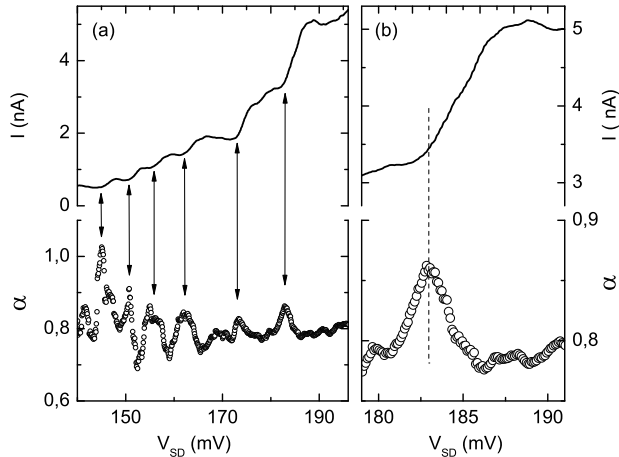


FIG. 4: (a) I - V characteristics of the sample at higher bias voltage (upper plot) in comparison with the measured Fano factor α (lower plot) for non-charging direction. The temperature was 1.7 K. The shot noise increases at every onset of a current plateau as indicated by the arrows. The plotted set of data for α has been smoothed using a 15-point boxcar average (the voltage resolution of the original data is $\Delta V_{SD} = 0.1$ mV). (b) Detailed plot of current (solid line) and corresponding Fano factor (open circles).

$I_{total}(V_{SD}) = \sum_{i=1}^{n(V_{SD})} I_i(V_{SD})$ with $n(V_{SD})$ being the number of transmitting QDs. As indicated by the dotted line in Fig. 1 each current $I_i(V_{SD})$ features an approximately linear decreasing behavior with increasing bias voltage.

From the theoretical models for on-resonance transport we know that the suppression coefficient α_i is constant and its value is given by Eq. (1). We may speculate that in the multi-dot regime the α_i are modified by additional mechanisms like interaction effects. The fluctuations in

the Fano factor minima may be traced to that. Nevertheless, this implies that with increasing bias voltage we have a growing number of QDs transmitting electrons with approximately constant value for the Fano factor α . Since we normalize the measured noise on the *total* current this results in a reduction of the effect of additional QDs coming into resonance.

In the limit of a large number of QDs being in resonance with the emitter Fermi sea we expect any modulation of the Fano factor to vanish, and its value to saturate at the value of the ensemble averaged suppression: $\langle \alpha \rangle = 1/n(V_{SD}) \sum_{i=1}^{n(V_{SD})} \alpha_i$. In fact, this is what we find for bias voltages above 190 mV, where $n(190 \text{ mV})$ is on the order of ten: The measured value $\alpha \approx 0.8$ is once again in reasonable agreement with the asymmetry of our tunneling structure (see above).

Apart from the main features found in the noise and I - V characteristics we observe a fine structure as shown exemplarily in Fig. 4 (b) around 181 mV. Most likely this can be linked to transport through QDs only weakly coupled to the emitter. Additionally, these fine structures may be influenced by the fluctuations of the local density of states in the emitter¹⁶.

To conclude, we have measured the shot noise of an array of self-assembled InAs quantum dots (QDs). We observe a suppression of the shot noise on current plateaus that is related to resonant tunneling through the zero-dimensional ground state of a QD as predicted by theory. In the step region between two current plateaus the noise increases. This is because of the negligible influence of the Pauli principle as long as the number of emitter electrons with the energy of a specific QD state is sufficiently low. As more QD states lie between the Fermi energy and the conduction band edge of the emitter we find a suppression of the modulation amplitude of the shot noise.

We acknowledge financial support from DFG, BMBF, DIP and TMR.

-
- * Electronic address: nauen@nano.uni-hannover.de
- ¹ A. Ambrozy, *Electronic Noise* (McGraw-Hill, 1982).
 - ² Y. P. Li, A. Zaslavsky, D. C. Tsui, M. Santos, and M. Shayegan, *Phys. Rev. B* **47**, 8388 (1988).
 - ³ H. C. Liu, J. Li, G. C. Aers, C. R. Leavens, M. Buchanan, and Z. R. Wasilewski, *Phys. Rev. B* **51**, 5116 (1995).
 - ⁴ L. Y. Chen and C. S. Ting, *Phys. Rev. B* **43**, R4534 (1991).
 - ⁵ J. H. Davies, P. Hyldgaard, S. Hershfield, and J. W. Wilkins, *Phys. Rev. B* **46**, 9620 (1992).
 - ⁶ Y. M. Blanter and M. Büttiker, *Phys. Rep.* **336** (2000).
 - ⁷ H. Birk, M. J. M. de Jong, and C. Schönberger, *Phys. Rev. Lett.* **75**, 1610 (1995).
 - ⁸ A. Nauen, J. Königmann, U. Zeitler, F. Hohls, and R. J. Haug, *Physica E* **12**, 865 (2002).
 - ⁹ G. Iannaccone, G. Lombardi, M. Macucci, and B. Pellegrini, *Phys. Rev. Lett.* **80**, 1054 (1998).
 - ¹⁰ V. V. Kuznetsov, E. E. Mendez, J. D. Bruno, and J. T. Pham, *Phys. Rev. B* **58**, R10159 (1998).
 - ¹¹ M. Narihiro, G. Yusa, Y. Nakamura, T. Noda, and H. Sakaki, *Appl. Phys. Lett.* **62**, 105 (1996).
 - ¹² I. E. Itskevich, T. Ihn, A. Thornton, M. Henini, T. J. Foster, P. Moriarty, A. Nogaret, P. H. Beton, L. Eaves, and P. C. Main, *Phys. Rev. B* **54**, 16410 (1996).
 - ¹³ T. Suzuki, K. Nomoto, K. Taira, and I. Hase, *Jpn. J. Appl. Phys.* **36**, 1917 (1997).
 - ¹⁴ I. Hapke-Wurst, U. Zeitler, H. Frahm, A. G. M. Jansen, and R. J. Haug, *Phys. Rev. B* **62**, 12621 (2000).
 - ¹⁵ I. Hapke-Wurst, U. Zeitler, H. W. Schumacher, R. J. Haug, K. Pierz, and F. J. Ahlers, *Semicond. Sci. Technol.* **14**, L41 (1999).
 - ¹⁶ T. Schmidt, P. König, E. McCann, V. I. Falko, and R. J. Haug, *Phys. Rev. Lett.* **86**, 276 (2001).